Nuclear Inst. and Methods in Physics Research, A 1055 (2023) 168377

Contents lists available at ScienceDirect

Nuclear Inst. and Methods in Physics Research, A

journal homepage: www.elsevier.com/locate/nima

Gain measurements on NLGAD detectors

Jairo Villegas [a,*], Neil Moffat [a], Dzmitry Maneuski [b], Oscar Ferrer [a], Giulio Pellegrini [a], Salvador Hidalgo [a]

[a] Instituto de Microelectrónica de Barcelona, IMB-CNM-CSIC, 08193 Cerdanyola del Vallès, Barcelona, Spain
[b] SUPA School of Physics and Astronomy, University of Glasgow, G12 8QQ, United Kingdom

ARTICLE INFO

Keywords:
LGAD
X-rays and charged particle detectors

ABSTRACT

In the last few years, Low Gain Avalanche Detectors (LGAD) have demonstrated their outstanding performance when detecting high-energy charged particles. However, due to the difference in the multiplication mechanism for holes and electrons, the detection performance for low penetrating particles (e.g low-energy protons or soft x-rays) is significantly reduced. A novel design of an LGAD detector, the NLGAD, was designed and fabricated at CNM to overcome this drawback. A qualitative description of the NLGAD concept is presented in this work, along with gain response measurements of the first prototypes under visible light of 660 nm and 15 keV x-rays. Additionally, a review of the gain response under visible light of 404 nm and IR light of 1064 nm, previously studied, is also evaluated in this work. The results demonstrate that the NLGAD concept has the potential to detect low penetrating particles.

1. Introduction

The first Low Gain Avalanche Detectors (LGAD) were designed and fabricated at the IMB-CNM [1]. Since then, the LGAD technology has been gradually established as the baseline for High Energy Physics experiments, including the upcoming ATLAS and CMS upgrade at the HL-LHC. Despite the ongoing work to increase their radiation hardness for high fluences, their outstanding timing resolution and SNR when detecting high energy particles have been demonstrated [2].

This excellent performance arises from the intrinsic charge multiplication mechanism, which is inherent to the LGAD design. A shallow p-type multiplication layer is diffused in between the N electrode and the high resistivity p-type bulk, which generates a high electric field around the junction when the detector is reverse biased (Fig. 1). Thus, any charge carrier generated by an impinging high-energy particle that traverses the high electric field region will have sufficient energy to cause impact ionization and hence avalanche multiplication. This increases the signal with respect to a standard PiN detector. The ratio between the generated charge by a particle in an LGAD and a standard PiN is the so-called gain.

However, there is a distinction between how electrons and holes trigger this avalanche multiplication mechanism. Therefore, the LGAD performance will be dependant on the depth at which the traversing particle generates the charge. In other words, it will depend on the impinging particle energy.

1.1. Avalanche multiplication for electrons and holes

The charge multiplication mechanism can be quantified with the impact ionization rate α, which is defined as the number of electron–hole pairs that a charge carrier generates by unit length at a given external electric field intensity. α is directly linked to mobility, a parameter that gives information about the probability of collision of a charge carrier with a silicon atom in the lattice (e.g. to cause ionization). It has been widely proven that the impact ionization rate (hence the mobility) is smaller for holes than electrons. An extensive analysis about this topic can be found in [3].

The fact that the electrons and holes mobilities are different arises from the very nature of the carriers. A conduction electron is excited from the outermost atomic shell of the silicon atom. The electron is free to move towards the N electrode under the influence of an external electric field and its motion is only perturbed by random collisions with the scattering centers in the silicon crystalline lattice. In contrast, the motion of a conduction hole starts when a Si-Si bond breaks and its electron occupies the vacancy left behind by the electron that first drifted. This bond breaking and vacancy occupation mechanism continues until the hole (a vacancy) has been pushed away from the active region of the detector to the P electrode. In short, both the drift of electrons and holes is caused by the motion of electrons, but in the case of holes they are not free. Transitioning between vacancy states is not as straightforward as freely drifting, hence holes have a lower collision probability than electrons.

* Corresponding author.
E-mail address: jairo.villegas@imb-cnm.csic.es (J. Villegas).

https://doi.org/10.1016/j.nima.2023.168377
Received 8 March 2023; Received in revised form 25 April 2023; Accepted 15 May 2023
Available online 12 June 2023

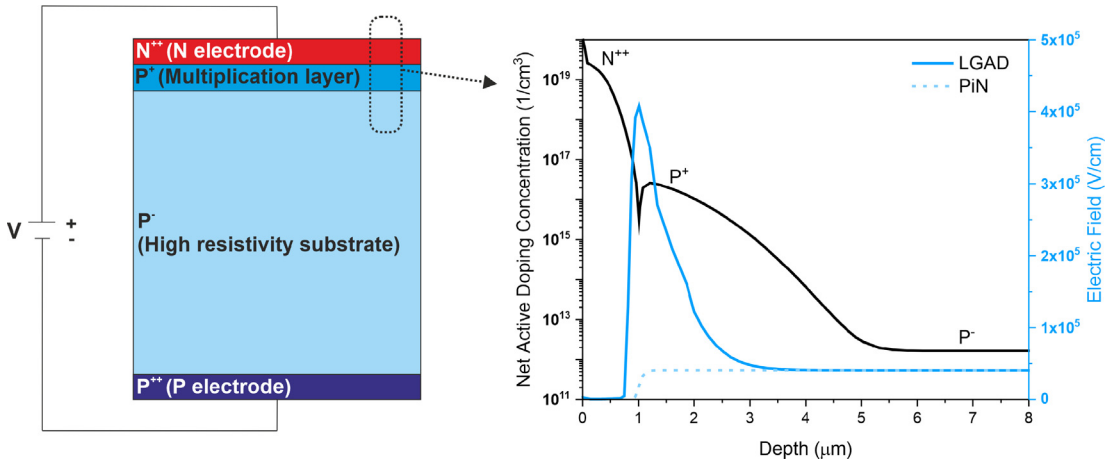

Fig. 1. Left: Basic schematics of the doped silicon layers in an LGAD. Right: TCAD simulation of the active doping concentration and electric field (at 250 V of reverse bias) of an LGAD and a PiN. The simulation served to design the LGADs on 6" epitaxial wafers fabricated at CNM and studied in [2].

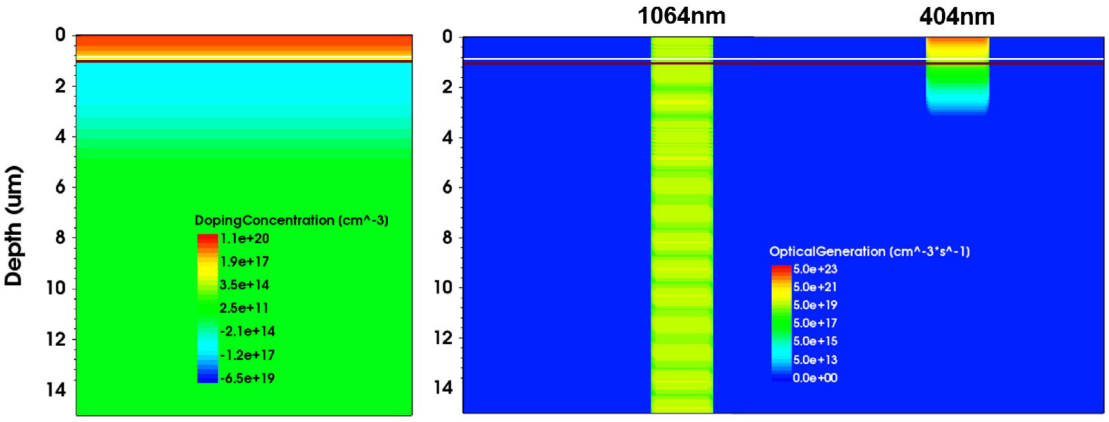

Fig. 2. TCAD simulation of active doping concentration (left) and optical generation by laser pulses of 404 and 1064 nm wavelength in a 50 μm LGAD (right). The laser pulses have the same intensity, duration and width in both cases. Pulses are injected through the N electrode. The horizontal brown line represents the $N^{++} - P^{+}$ junction, where the electric field is at its maximum. The pictures have been cut at a depth of 15 μm to clearly remark the gain layer and the optical generation for 404 nm light.

One could conclude that the gain of an LGAD in response to incident ionizing radiation will depend on the depth at which the particles are most likely depositing their energy, as this will determine which charge carrier (electrons or holes) is the primary contributor to trigger avalanche multiplication. The gain response of an LGAD when traversed by photons of 404 nm and 1064 nm will be evaluated.

Photons in this energy range interact with silicon mainly via the photoelectric effect, so, unlike charge particles, they give up all their energy to generate a single $e^{-} - h^{+}$ pair. Fig. 2 shows the TCAD simulation of the optical generation (average $e^{-} - h^{+}$ pairs generated by volume and unit time) when an LGAD is illuminated through the N electrode (Fig. 1) by identical laser pulses (in terms of intensity, duration and width) of 404 nm and 1064 nm wavelength. The optical generation is proportional to the photoabsorption probability at a given depth.

A photon of 1064 nm, with an absorption depth of $\sim$ 1000 μm in silicon [4], will be absorbed in any depth of the 50 μm LGAD with the same probability (Fig. 2). Thus, the IR pulse will generate a uniform distribution of $e^{-} - h^{+}$ pairs within the active depth of the detector. Under these circumstances, there will be a greater number of electrons crossing the high electric field region, so they will be the main carrier contributing to the avalanche mechanism triggering.

However, a visible photon of 404 nm, with an absorption depth of ~ 0.1 μm in silicon [4], will be either absorbed within the N electrode (not causing any detectable signal) or close to the $N^{++} - P^{+}$ junction. In this latter situation, most of the electrons will quickly drift to the N electrode without traversing the high electric field region. This will mean that the majority of charge carriers crossing the high field region will be holes.

With all that said, we could hypothesize that the gain response of a LGAD upon impinging 404 nm photons is diminished in contrast to the 1064 nm one. This result was predicted by means of TCAD simulation and confirmed by TCT (Transient Current Technique [5]) measurements at CNM, as Fig. 3 shows.

The same stands for charged particles. If they have a low range in silicon ($\lesssim$ 1 μm) and deposit most of their energy in the surface (close to the N^{++}/P^{+} junction), holes are expected to be the main contributor to cause impact ionization, hence the gain response of a LGAD will be reduced.

2. The NLGAD concept

A good gain response of an LGAD is limited to high penetrating particles, that is, to highly energetic charged particles (e.g. MIP) and photons with a high wavelength . For low penetrating particles, a new design of LGAD is necessary: the NLGAD. The design features of an NLGAD are similar to the ones described in Fig. 1 for a traditional LGAD, with the difference that the dopant type is exchanged in every one of its silicon layers (Fig. 4): a shallow n-type multiplication layer is diffused between the P electrode and the high resistivity n-type bulk, creating a high electric field around the $P^{++} - N^{+}$ junction when the detector is reverse biased.

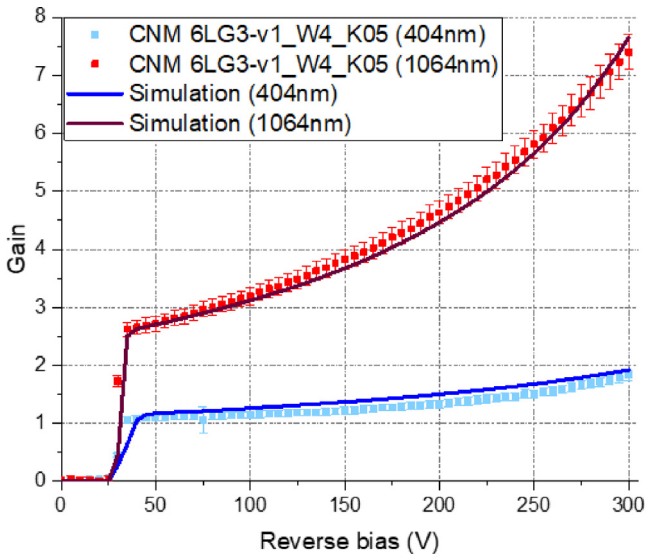

Fig. 3. TCT measurements and TCAD simulation of the gain response, at room temperature (20 °C), of an LGAD fabricated with the CNM-6LG3 (LGADs on epitaxial wafers of 6") technology, for two different laser wavelengths: 404 nm and 1064 nm. It is worth mentioning that the intensity of the laser pulses during the TCT measurements was different for 404 and 1064 nm light to avoid saturation of the amplifier. However, the intensity was kept at a sufficient low value to avoid gain suppression [6].

As in the case of the traditional LGAD, the first NLGADs were designed, fabricated and tested at IMB-CNM [7].

Since electrons and holes are drift in opposite directions compared to a traditional LGAD, for an NLGAD it is expected that the gain response is higher for the low penetrating 404 nm photons than for the 1064 nm ones. This hypothesis was confirmed by TCT measurements, which showed that the gain for 404 nm photons was close to 10 times higher than for 1064 nm photons [7].

3. NLGAD gain response to photons of different energy

The NLGADs were fabricated at the IMB-CNM on 4" n-type high resistivity Si-Si wafers (CNM-4NLG1 technology). The devices have an active area and thickness of 5.3 × 5.3 mm^2 and 275 μm, respectively. They have a full depletion voltage of ≃ 30 V, a breakdown voltage of ≃ 170 V (at room temperature) and their leakage current in the operational voltage region is of the order of 100 nA. Their electrical characterization can be found in [7].

Detectors of this first NLGAD production were tested for visible (404 nm) and IR light (1064 nm), where a higher gain response was shown for the 404 nm case [7]. In this work the characterization of such NLGADs is extended to photons of different energy and type: visible light of 660 nm and X-ray photons of 15 keV. In both cases, the measurements were carried out focusing the beam close to the center of the devices, at room temperature (≈20 °C) and up to 120 V (≈50 V away from breakdown). Fig. 6 shows the absorption depth (inverse of the attenuation coefficient) for these photon energies [4,8]. As evaluated in the previous section and demonstrated by the results in [7], it is expected that the NLGAD gain is higher (at a given reverse bias) for 660 nm visible light with respect to 15 keV X-rays, given their absorption depth in silicon.

3.1. The importance of the entrance window for very low penetrating particles

TCT measurements using a pulsed UV laser of wavelength 369 nm were also performed in NLGADs and reference PiN devices, however no signal response could be seen. This result highlights the importance of having a thin entrance window for low penetrating particles detectors, as pointed out in [7]. Devices from the CNM Run 4NLG1-v1 have a non active layer (passivation plus SiO_2) of ≈ 1 μm, thick enough to completely attenuate 369 nm UV photons, which absorption depth is of the order of 10 nm in silicon (Fig. 6).

3.2. TCT measurements: Gain response to visible light (660 nm)

An NLGAD detector from the CNM Run 4NLG1-v1 was investigated for its gain response while illuminated by 660 nm visible light. The measurements were carried out at room temperature with a TCT setup [5]. The laser beam (with a beamspot of the order of 10 μm) was focused around the center of the device. Such center was found by scanning the devices in X and Y using steps of 100 μm. The laser pulse intensity, frequency and width were kept constant for both NLGAD and reference PiN during the measurements. The gain was calculated by dividing the integrated amplified output signal (Fig. 7), for every reverse bias point, of the NLGAD by the PiN one.

3.3. Measurements at diamond light source: Gain response to 15 keV X-rays

Measurements were carried out at the B16 beamline available at Diamond Light Source [9]. With the use of a crystal monochromator, this beamline is able to provide monochromatic X-ray beams in the range of 4–45 keV out of synchrotron radiation. Also, a compound refractive lens (CRL) was used in the beamline to obtain a microfocused X-ray beam with a spot size of a few μm. The beam spot size was found to be 2.6 ± 0.1 μm FWHM (X direction) and 1.3 ± 0.1 μm FWHM (Y direction). The projection of the beam around the center of the devices,

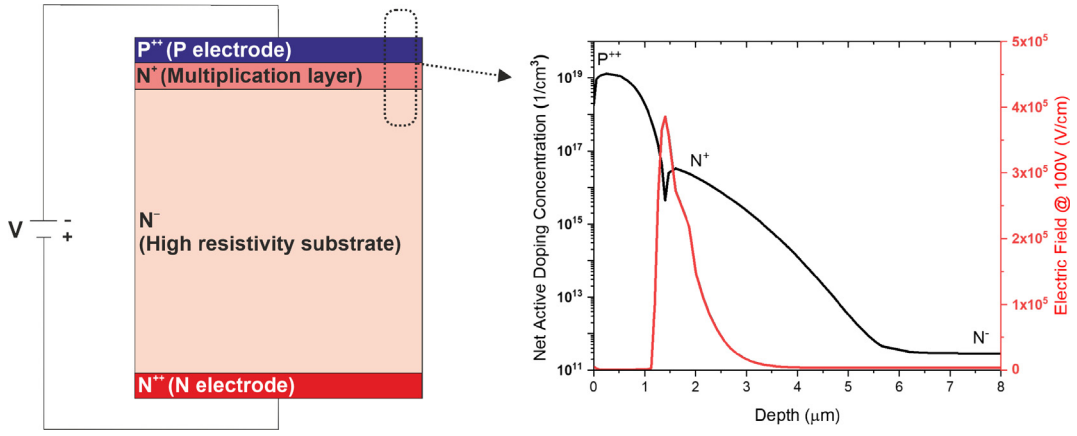

Fig. 4. Left: Basic schematics of the doped silicon layers in an NLGAD. Right: TCAD simulation of the active doping concentration and electric field (at 100 V of reverse bias) of an NLGAD. The simulation served to design the NLGADs fabricated at CNM and studied in this paper.

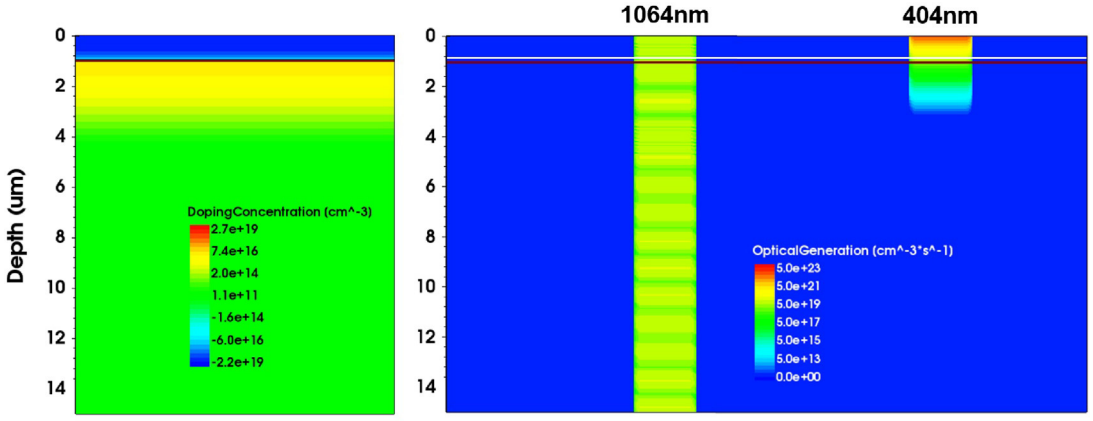

Fig. 5. TCAD simulation of active doping concentration (left) and optical generation by laser pulses of 404 nm and 1064 nm wavelength in a 275 μm NLGAD (right). The laser pulses have the same intensity, duration and width as in Fig. 2. Pulses are injected through the P electrode. The horizontal brown line represents the P^{++}/N^{+} junction, where the electric field is at its maximum. The pictures have been cut at a depth of 15 μm to show clearly the gain layer and the optical generation for 404 nm light.

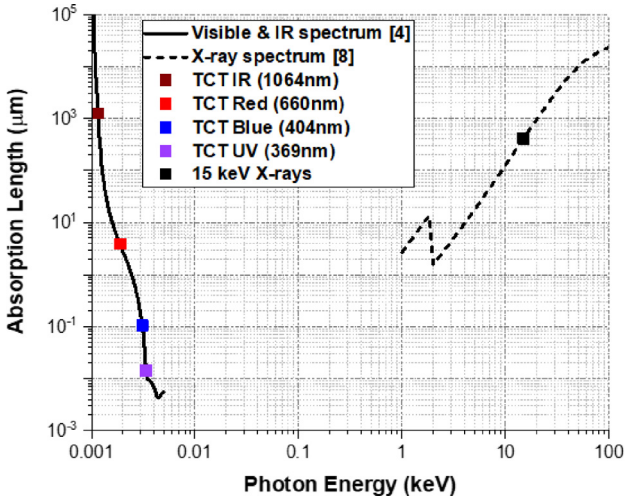

Fig. 6. Absorption length for photons in the energy range of IR, visible light and X-rays [4,8].

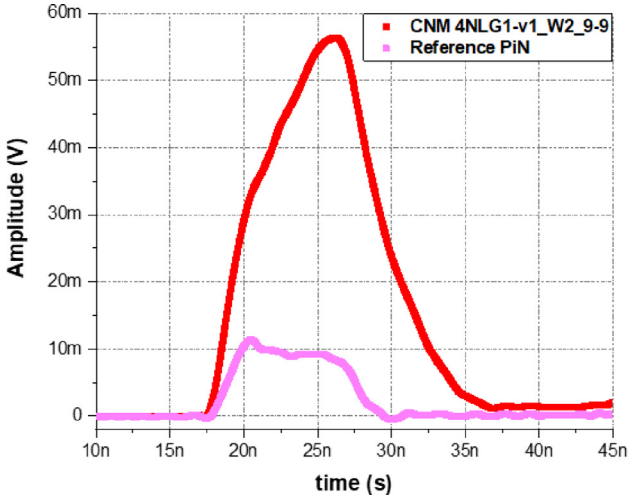

Fig. 7. TCT output signal for the studied NLGAD and reference PiN under illumination with 660 nm visible light, at 100 V reverse bias and room temperature (20 °C). For every reverse bias point, the TCT output signal is composed of 5000 averaged waveforms.

mounted perpendicularly to the X-ray beam direction, was achieved with the help of a visible laser available at the experimental hutch of the beamline. The beam intensity was controlled at all times by an ionization chamber composing the beamline setup. In contrast to the TCT case, the gain of the NLGAD device is not evaluated by illumination with short light pulses, but with a beam of X-rays in continuum. Thus, the gain was calculated by dividing the photocurrent (defined as the current generated in the device, when depleted and with the X-ray beam focused on the center, minus the leakage current) of the NLGAD by the one of the reference PiN. The current was measured with a Keithley 2410, taking 20 measurements per voltage step (Fig. 8).

3.4. Gain response and simulation

Fig. 9 shows the gain response results for 660 nm visible light and 15 keV X-rays, using the two different techniques and gain evaluation methods described in the above paragraphs, along with TCAD simulations. As in Fig. 3, the simulated gain has been obtained by using the Van Overstraeten De Man avalanche model [3] to detectors (NLGADs and PiNs) with a doping profile optimized to predict the electrical characterization of devices fabricated at the IMB-CNM clean room.

4. Conclusions

The studies presented in this work demonstrate that the gain response of a NLGAD is higher for visible light of 660 nm than for 15 keV X-rays. Fig. 11 presents a comparison of gain measurements, obtained illuminating the NLGADs from the CNM Run 4NLG1-v1 with photons of different energies, combining the TCT measurements presented in this work with the ones presented in [7].

The results demonstrate that the novel NLGAD may be suitable for experiments that imply detection of low penetrating charged particles (some of them are listed in ref [7]) and soft X-rays, such as synchrotron applications.

Also, the unresponsiveness for UV light of 369 nm wavelength highlighted the importance of reducing the non-active layers of the entrance window for future designs. A good example of it can be found in [10]: by creating the PN junction utilizing single layer graphene, UV light down to 200 nm wavelength could be detected by silicon sensors.

CRediT authorship contribution statement

Jairo Villegas: Simulation, Detectors X-ray Irradiation and measurements, TCT Measurements, Formal analysis, Investigation, Data curation, Validation, Writing – original draft, Writing – review & editing. **Neil Moffat:** Simulation, Detectors X-ray Irradiation and measurements, Investigation, Writing – review & editing. **Dzmitry Maneuski:** Detectors X-ray Irradiation and measurements, Formal analysis. **Oscar**

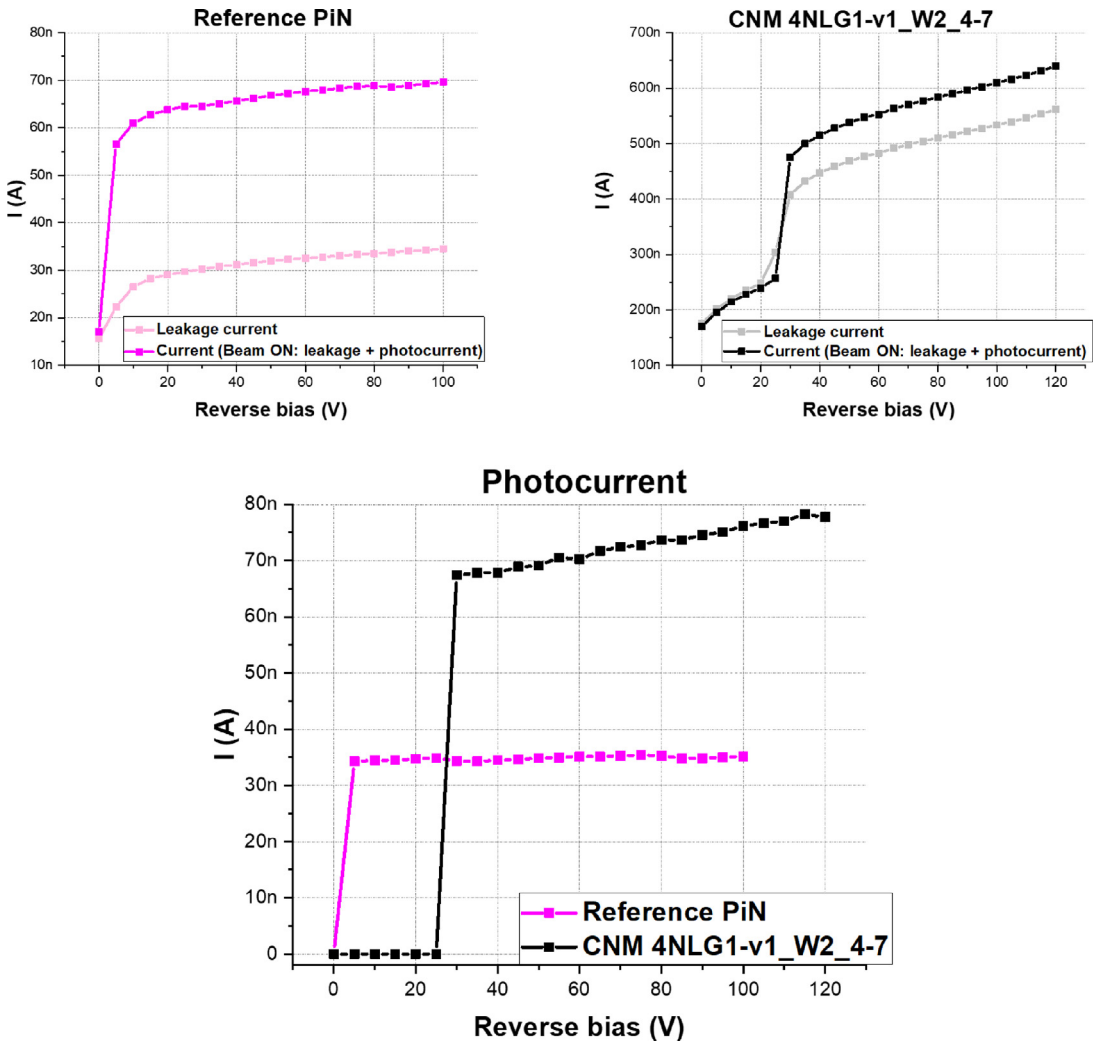

Fig. 8. Leakage current and current under irradiation with a micro-focused 15 keV X-ray beam for the tested NLGAD and reference PiN. The photocurrent for each case is calculated by subtracting the leakage current to the current under irradiation for every voltage step over the depletion voltage (30 V for the NLGAD, 5 V for the reference PiN).

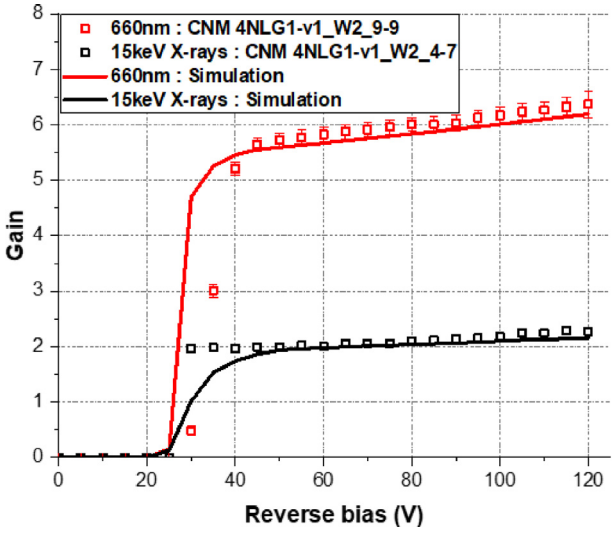

Fig. 9. Gain response of NLGADs from the CNM Run 4NLG1-v1 to 660 nm visible light and 15 keV X-rays.

Ferrer: TCT Measurements. **Giulio Pellegrini:** Detectors X-ray Irradiation and measurements, Conceptualization, Methodology, Validation, Resources, Funding acquisition. **Salvador Hidalgo:** Conceptualization, Methodology, Validation, Resources, Data curation, Writing – review & editing, Work Supervision, Project administration, Funding acquisition.

Declaration of competing interest

The authors declare the following financial interests/personal relationships which may be considered as potential competing interests: Jairo Antonio Villegas Dominguez reports financial support, administrative support, article publishing charges, equipment, drugs, or supplies, statistical analysis, and travel were provided by Spanish Scientific Research Council. Jairo Antonio Villegas Dominguez reports a relationship with Spanish Scientific Research Council that includes: employment, funding grants, non-financial support, and travel reimbursement.

Data availability

Data will be made available on request.

Acknowledgments

This work has been funded by the Spanish Ministry of Science and Innovation (MCIN/AEI/10.13039/501100011033/) and by the

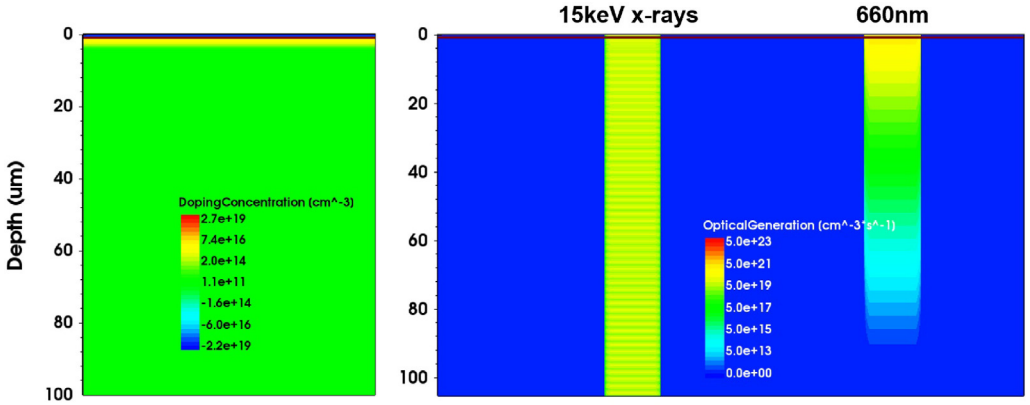

Fig. 10. TCAD simulation of active doping concentration (left) and optical generation by pulses of 660 nm wavelength and 15 keV X-rays in an NLGAD (right). Laser illumination features are the same as the ones described in Fig. 3.

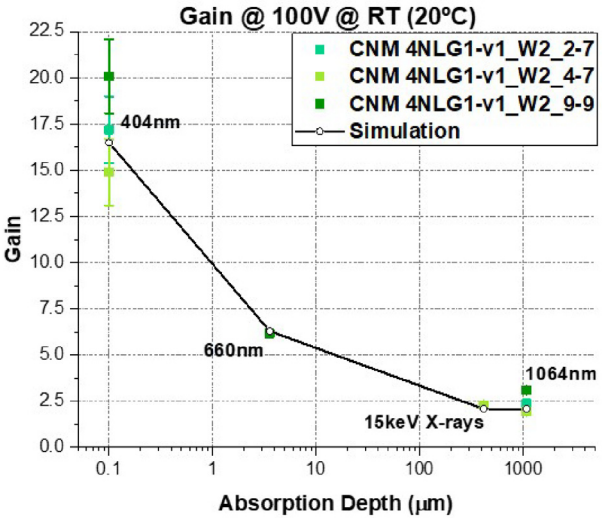

Fig. 11. Gain response, at 100 V and at room temperature, of NLGADs from the CNM Run 4NLG1-v1. The gain is presented against absorption depth for every photon energy/wavelength, to have a better comparison with the depth features of the device. To avoid saturation of the output amplifier signal when measuring the NLGAD response for the 404 nm light, the width of the laser was reduced. This also decreased the SNR when measuring the PiN response, increasing the error associated to the gain measurement for this wavelength.

European Union's ERDF program "A way of making Europe". Grant references: RTI2018-094906-B-C22 and PID2020-113705RB-C32. Also, it was funded by the European Union's Horizon 2020 Research and Innovation funding program, under Grant Agreement No. 101004761 (AIDAInnova). The authors would also like to thank Vishal Dhamgaye, Oliver Fox and Kawal Sawhney, personnel of the B16 beamline of Diamond Light Source, for providing support and maintenance during the experiments.

References

[1] G. Pellegrini, et al., Technology developments and first measurements of Low Gain Avalanche Detectors (LGAD) for high energy physics applications, Nucl. Instrum. Methods Phys. Res. A 765 (2014) 12–16.
[2] C. Grieco, et al., Overview of CNM LGAD results: Boron Si-on-Si and epitaxial wafers, J. Instrum. 17 (2022) C09021.
[3] R. Van Overstraeten, H. de Man, Measurement of the ionization rates in diffused p-n junctions, Solid-State Electron. 13 (5) (1970) 538–608.
[4] M.A. Greens, M.J. Keevers, Optical properties of intrinsic silicon at 300K, Photovoltaics 3 (3) (1995) 189–192.
[5] N. Moffat, Low Gain Avalanche Detectors for Particle Physics and Synchrotron Applications (PhD thesis), School of Physics and Astronomy, Glasgow, 2020, Unpublished.
[6] E. Curras, et al., Gain suppression mechanism observed in low gain avalanche detectors, 2021, arXiv:2107.10022v1.
[7] W. Khaled, et al., First results for the pLGAD sensor for low-penetrating particles, 2022, arXiv:2207.06047.
[8] J.H. Hubbell, S.M. Seltzer, Tables of X-ray mass attenuation coefficients and mass energy-absorption coefficients from 1keV to 20MeV for elements Z=1 to 92 and 48 additional substances of dosimetric interest, 1995, NISTIR 5632.
[9] Diamond light source. B16 Beamline website (online): https://www.diamond.ac.uk/Science/Research/Optics/B16.html.
[10] N. Moffat, et al., Graphene-enabled silicon-integrated photodiode for DUV imaging, in: IEEE 22nd International Conference on Nanotechnology, NANO, 2022, pp. 120–123, http://dx.doi.org/10.1109/NANO54668.2022.9928637.